Distribution Agreement

In presenting this thesis or dissertation as a partial fulfillment of the requirements for an advanced degree from Emory University, I hereby grant to Emory University and its agents the non-exclusive license to archive, make accessible, and display my thesis or dissertation in whole or in part in all forms of media, now or hereafter known, including display on the world wide web. I understand that I may select some access restrictions as part of the online submission of this thesis or dissertation. I retain all ownership rights to the copyright of the thesis or dissertation. I also retain the right to use in future works (such as articles or books) all or part of this thesis or dissertation.

Signature:

_____   _____
Shawnna Joynt   Date

Globin Coupled Sensor Signaling in *P. carotovorum*:
A Model of Biofilm Regulation through Oligomerization of Diguanylate Cyclases

By

Shawnna Joynt
Master of Science

Chemistry

_____
Emily Weinert, Ph.D.
Advisor

_____
Vincent Conticello, Ph.D.
Committee Member

_____
Stefan Lutz Ph.D.
Committee Member

Accepted:

_____
Lisa A. Tedesco, Ph.D.
Dean of the James T. Laney School of Graduate Studies

_____
Date

Globin Coupled Sensor Signaling in *P. carotovorum*:
A Model of Biofilm Regulation through Oligomerization of Diguanylate Cyclases

By

Shawnna Joynt
B.S., Florida State University, 2011

Advisor: Emily Weinert, Ph.D.

An abstract of
A thesis submitted to the Faculty of the
James T. Laney School of Graduate Studies of Emory University
in partial fulfillment of the requirements for the degree of
Master of Science
in Chemistry
2013

Abstract

Globin Coupled Sensor Signaling in *P. carotovorum*:
A Model of Biofilm Regulation through Oligomerization of Diguanylate Cyclases

By Shawnna Joynt

Bacterial infestation of plants by *Pectobacterium carotovorum ssp carotovorum* (*P. carotovorum*), commonly called soft rot, creates world-wide devastation of many crops. Studies have shown that *P. carotovorum* grows rapidly in a more hypoxic state and becomes less virulent in aerobic environments. These studies, however, do not consider how oxygen may be involved in regulating virulence by switching the bacteria from an actively growing state to a sessile biofilm and whether that switch is due to oxygen sensitive globin coupled sensors (GCS). Diatomic gases can bind to the heme domain within a GCS to activate or turn-off the protein's catalytic domain. GCSs with diguanylate cyclase activity studied to date produce the secondary signaling molecule bis-(3'-5')-cyclic diguanosine monophosphate (c-di-GMP), which is positively associated with biofilm growth. Therefore, we hypothesize that a globin coupled sensor within *P. carotovorum* (*Pcc*GCS) has a direct role in the regulation of biofilm formation. This study characterizes the basic biochemical properties and mechanism of *Pcc*GCS regulation. We show that *Pcc*GCS is an active response regulator that may use its globin domain to induce dimerization and subsequent activation of its diguanylate cyclase domain.

Globin Coupled Sensor Signaling in *P. carotovorum*:
A Model of Biofilm Regulation through Oligomerization of Diguanylate Cyclases

By

Shawnna Joynt
B.S., Florida State University, 2011

Advisor: Emily Weinert, Ph.D.

A thesis submitted to the Faculty of the
James T. Laney School of Graduate Studies of Emory University
in partial fulfillment of the requirements for the degree of
Master of Science
in Chemistry
2013

Table of Contents

Index of Figures

Introduction

P. carotovorum Infection

Infestation of crops by *P. carotovorum* creates world-wide devastation of many harvests, causing hundreds of millions of dollars in yearly crop loss world wide.[1] The wide variety of plants affected by soft rot is due to the bacteria's ability to break down its host's cell wall through excretion of pectinases and other cell wall-hydrolyzing enzymes.[2] This mechanism allows facile accessibility to feed and grow on the plant's nutrients, giving infected plants distinguishable soft, black spots. Another contributing factor to the pathogen's wide-spread infection is its ability to target plants at any stage of development.[3] The bacteria may infect a plant while it is still a seed, while it is developing, or after harvest. Due to close proximity, the most susceptible environment for widespread damage is after harvest within storehouses.[4] Once a single infected plant enters a warehouse, it can easily spread throughout the entire harvest.

Studies have found that soft rot grows best in wet, anaerobic environments.[5, 6] Therefore, many storehouses are supplemented with a higher oxygen atmosphere.[7, 8] Other prevention methods include minimizing mechanical damage to the crop, avoiding planting seeds in excessively moist soil, and drying the harvest before storage. Though these methods are effective, there is no sure-proof way of preventing soft rot. Infections continue to destroy many harvests, the majority of which are in economically disadvantaged areas that cannot afford the high quality water and storage houses necessary for soft rot prevention.[3] Given the widespread effect and devastation of *P. carotovorum* infection, ongoing research is necessary to develop new improvements in soft rot containment.

This study focuses on understanding the role of oxygen in decreasing the virulence of the soft rot pathogen. Since many plants require oxygen for structurally sound cell membranes and contain oxygen-dependent defenses against bacteria, *P. carotovorum* benefits from being able to thrive in an anaerobic state.[3] However, a correlation between reduced virulence in an aerobic environment with the activation of a diguanylate cyclase has not been studied. Since activation of diguanylate cyclase (DGC) domains initiate biofilm formation and decrease virulence, studying *Pcc*GCS will provide an explanation of oxygen's influence on *P. carotovorum*'s overall pathogenicity. [9, 10]

Diguanylate Cyclase Domains

Recent attention has been brought to diguanylate cyclase domains for their ability to directly synthesize c-di-GMP from two GTP molecules.[10] Regulation of c-di-GMP concentration is imperative for the cell since this secondary signaling molecule is positively associated with biofilm formation.[9, 11] A general scheme is displayed in Figure 1.[12] Each monomer can bind one GTP molecule.[13] Therefore, c-di-GMP is synthesized when two domains dimerize, allowing cyclization at the monomer interface.[14] Since diguanylate cyclases are typically associated with a sensing domain that controls its activity, we hypothesize that the affiliated sensing domain may control activity through oligomerization. We further propose that globin coupled sensors with diguanylate cyclase domains influence oxygen sensitive biofilm formation in a number of pathogens. Though this study focuses on the diguanylate cyclase from *P. carotovorum*, the proposed mechanism of biofilm regulation may also reflect that of *E. coli* and *B. pertussis*, the causative agent of whooping cough.[15]
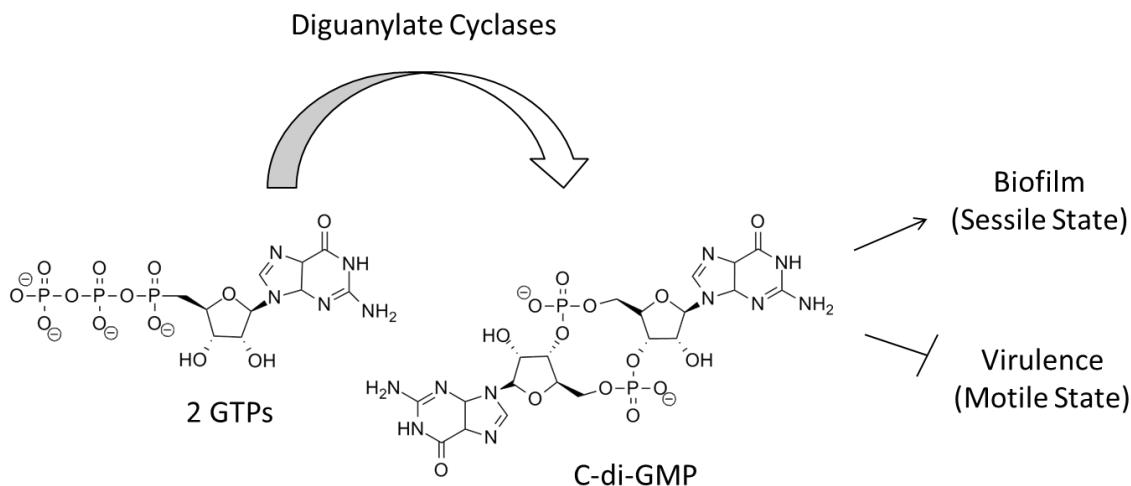
Figure 1: Two GTP molecules are converted to c-di-GMP through diguanylate cyclase activity. C-di-GMP is positively associated with biofilm formation.[12]

Heme-Binding Signal Transducers

Heme-based sensing proteins give bacteria an advantage for adapting to environmental factors by directly responding to the presence of certain diatomic gases.[16] These signal transducers contain an N-terminal input domain and a C-terminal catalytic domain connected by a middle domain of unknown function, as seen in Figure 2.[17] To qualify as a signal transducer, the sensing domain must directly control the activity of the output. Therefore, heme-binding sensing domains are a new class of heme motifs designed to distinguish between gaseous ligands, rather than for gas delivery or catalysis.[18] A number of heme sensory domains exist, such as the PAS, CooA, and H-NOX domains.[16] Output domains also consist of a wide variety of activities, such as DNA binding, secondary messenger synthesis (diguanylate cyclases), methyl carrying, and phosphorylation.[19] This study will focus on a new type of heme-based sensing family, termed globin coupled sensors (GCSs).[17, 20] Although GCSs are predicted to have

a number of varying catalytic domains, this work focuses on a GCS with diguanylate cyclase activity.
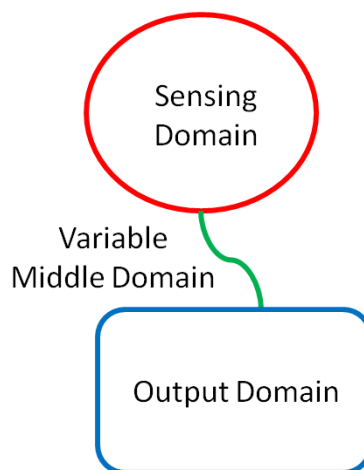
Figure 2: General schematic of heme-binding signal transducers, which contain a heme-bound sensing domain, a catalytic output domain, and a middle linker domain.[17]

Globin Coupled Sensors

Globin coupled sensors (GCS) are a relatively new group of heme-binding signal transducers. GCS sensory domains contain a heme cofactor that is very similar structurally and spectroscopically to myoglobin.[18] The heme domain allows bacteria to sense various diatomic gaseous ligands, such as oxygen, carbon monoxide, and nitric oxide in the environment.[16] Globin coupled sensors can also have numerous receiver domains; the most well studied are methyl-accepting chemotaxis transducers and diguanylate cyclase domains.[19] Methyl-accepting chemotaxis transducers allow the bacteria to control its flagella in order to move away from toxic gasses or chemicals.[21] Since globin coupled sensors are relatively new, very few have been characterized and even fewer sensors with diguanylate cyclase domains have been studied. To date only *Ec*DosC,[22] *Bpe*Greg,[15] *Av*GReg,[23] and HemDGC[24] have been investigated, and all were found to be activated by oxygen. This study expands this list to include *Pcc*GCS and

contributes a to a better understanding of these sensors in general. A homology model of a globin coupled sensor from *B. pertussis* is shown in Figure 3. Though the model has high homology between the globin and DGC domains, there is no structural similarity among the middle domains. This demonstrates that the conserved domains are essential for activity, but that the linker domain can be variable.
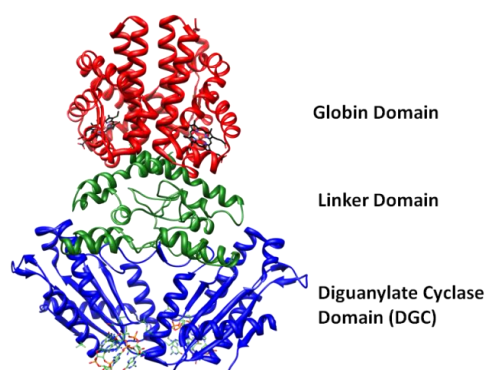
Figure 3: Homology model of GCS with DGC activity domain. Model is based on PDBs 10R4 and 3BRE.

Though globin coupled sensors may have a significant role in bacterial metabolic regulation, the mechanism of GCS communication has yet to be determined. This family of proteins is self-regulated through a complex, dynamic communication between three internal domains.[18] A number of studies have proposed differing conformations of the hydrogen bonding network within the heme pocket, however these studies do not explain the signal transfer between the globin and output domains.

When oxygen binds to the heme pocket, an altered conformation of the pocket should propagate a rearrangement that is different from the binding of other diatomic gases. If this rearrangement were primarily dependent on proximal strain between the iron and histidine, such as hemoglobin,[25] then differing gasses may not be distinguished

since both CO and O_2 form similar 6-coordinate heme complexes. To this end, the rearrangement of HemAT's distal pocket has been widely studied.
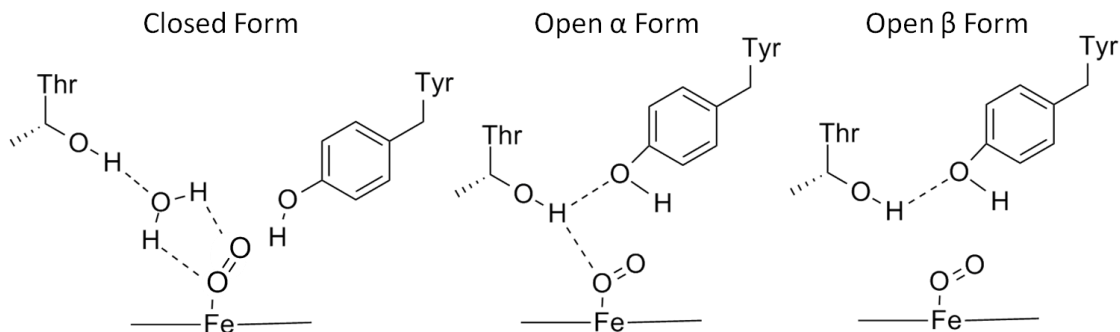
Figure 4: Proposed hydrogen bonding of globin's closed and two open conformations. Activation of the open form is suspected to disrupt a structural connection with the middle and catalytic domains.[28]

HemAT proteins, responsible for aerotaxis in *Bacillus subtilis* and *Halobacterium salinarum*, are globin coupled sensors with methyl-accepting chemotaxis receivers. Therefore, oxygen binding at the heme controls flagellar motion rather than DGC activity.[21] HemeAT studies show that distal pocket hydrogen bonding in globin coupled sensors have a significant role in differentiating ligands through a conserved tyrosine and threonine (serine in some proteins).[26] Resonance Raman spectroscopy has shown that one closed and two open conformations can exist when oxygen is bound to the heme, as seen in Figure 4.[27] However, only the open conformations exist when CO is bound. Site-specific mutagenic characterization of these homologous residues suggest that the distal threonine is necessary for the sensing of bound oxygen, while the distal tyrosine is essential for signal communication with the catalytic domain.[27] It was also found that the closed structure disappears in the Raman spectra of a truncated mutant missing the linker and catalytic domains. The disappearance of the closed conformation in this truncated

mutant indicates that closed form has a structural connection to the middle and catalytic domain.[27]

These studies propose how the rearrangement of the heme pocket may change upon ligand binding. However, they do not provide a mechanism for how this rearrangement induces catalytic activity. Diguanylate cyclases, such as the CheY phospho-receivers PleD and WspR, have been shown to be active as a homodimers and inactive as tetramers.[28, 29] This is logical since two GTPs are required to form one c-di-GMP. However, these studies are intriguing because they go on to demonstrate that the dimeric conformation is triggered by activation of the sensing domain and that the inactive oligomers are spurred by allosteric binding of c-di-GMP.[30, 31] Therefore, we propose that globin coupled sensors with diguanylate cyclase activity may also be regulated through association of oligomeric states. We further hypothesize that oxygen binding in the sensing domain may induce active dimer formation.

Since globin coupled sensors may have a great effect on the formation of biofilms across many bacterial species, elucidating the GCS mechanism would provide a better understanding of biofilm regulation not only for soft rot pathogens but also for pathogens infecting human hosts.[15] This study will produce an in-depth investigation of the communication between the globin and diguanylate cyclase domains of *Pcc*GCS through oligomerization states. Elucidating the effects of oligomerization on *Pcc*GCS activity will demonstrate a fundamental understanding of the GCS mechanism as well as provide groundwork for creating novel approaches in the artificial formation or dispersal of biofilms.

Results and Discussion

Discovery of and Activity of *Pcc*GCS

Sequence Alignment

Predicted homologous globin coupled sensors with diguanylate cyclase activity share many distinctive features. Each protein is approximately 500 amino acids long and has a high consensus with other GCS, particularly in the globin and diguanylate cyclase domains.[19] Though many residues vary, a number of residues required for heme binding and activity are conserved. As highlighted in Figure 5, these residues include a distal tyrosine and proximal histidine required for heme and ligand binding, respectively. Within the DGC domain, a GG(D/E)EF motif is required for DGC activity and an RXXD motif propagates allosteric product inhibition.[19] Through such highly conserved residues,
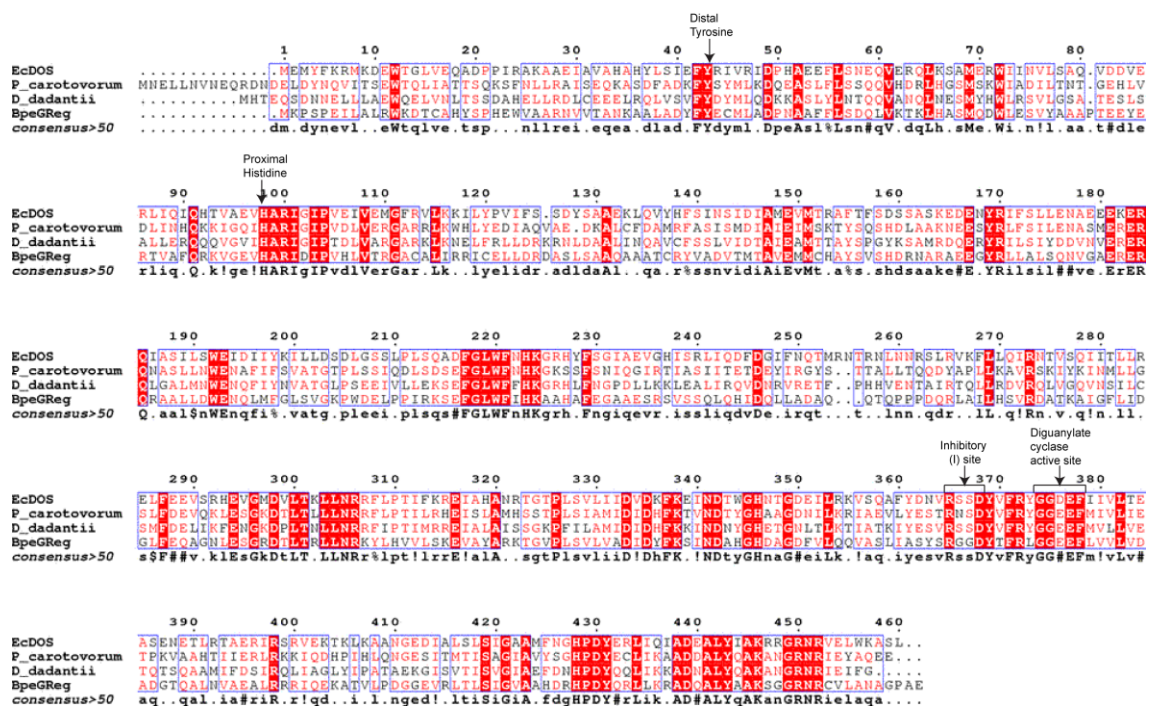
Figure 5: Sequence Alignment of homologous Globin Coupled Sensors
Homologous GCS from *E. coli, P. carotovorum, D. Dadantii, B. pertussis* is displayed.
The distal tyrosine, proximal histidine, inhibitory site, and diguanylate cyclase active site are also highlighted.

a globin coupled sensor, *Pcc*GCS, was predicted by BLAST to exist within *P. carotovorum* (YP_003018185.1). Following identification through a bioinformatics search, the DNA sequence was synthesized and cloned by GeneScript into a heterologous cloning vector with an N-terminal His tag and Factor Xa protease recognition site. The protein was then expressed and purified by Ni-NTA affinity chromatography.

Initial Characterization

Following *Pcc*GCS expression and purification, incorporation of heme was assayed by UV-Vis spectroscopy (Cary 100 UV-Vis spectrometer). Each ligation state has a characteristic UV-Vis spectra, with a soret from 390-435 nm and alpha beta bands around 550-600nm. The ferrous-unligated, ferrous-oxy, ferrous-CO, ferrous-NO, ferric, and ferric-CN states were successfully constructed, as seen in Figures 6, 7, and 8. Detection and differentiation of the ligation states by UV-Vis spectroscopy demonstrated that the purified protein contains functioning heme that can bind all of the reported gaseous ligands involved in globin coupled sensor signaling.
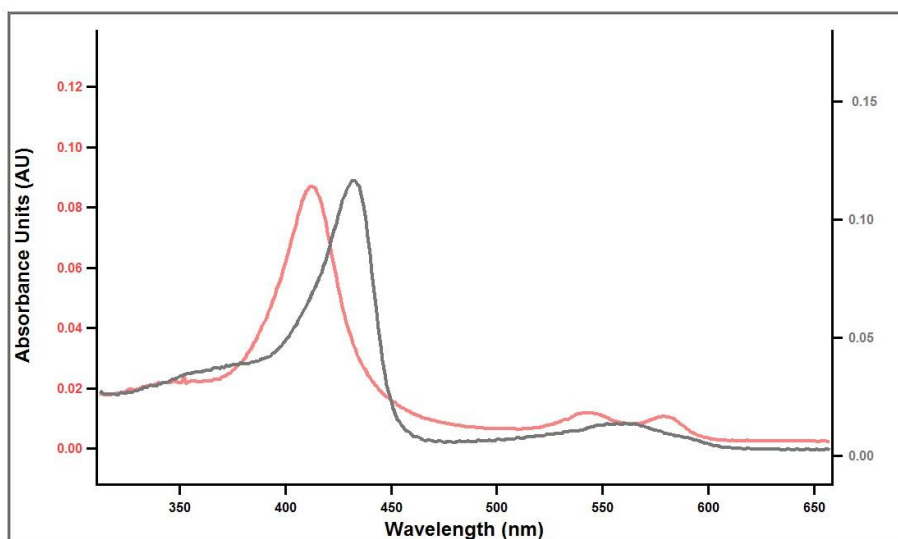
Figure 6: UV-Vis spectroscopy of *Pcc*GCS in the ferrous-oxy (red) and ferrous-unligated (black) states.
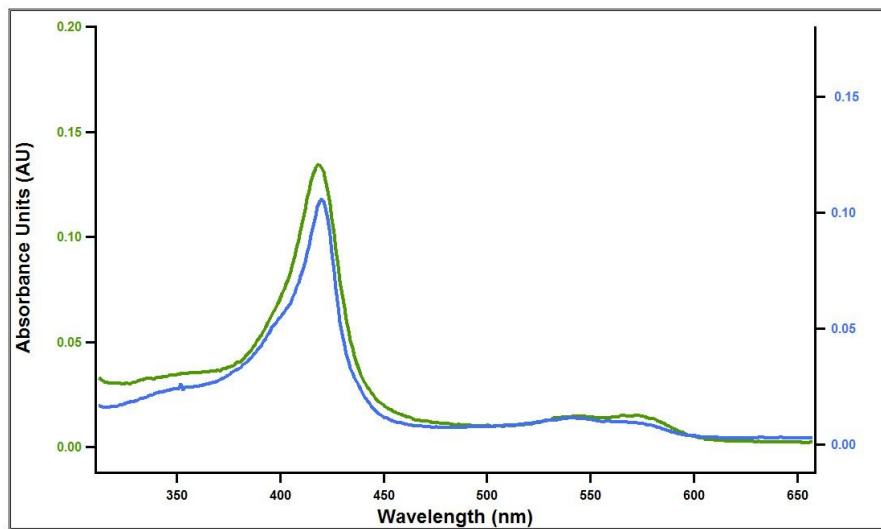
Figure 7: UV-Vis spectroscopy of *Pcc*GCS in the ferrous-CO (blue), and ferrous-NO (green).
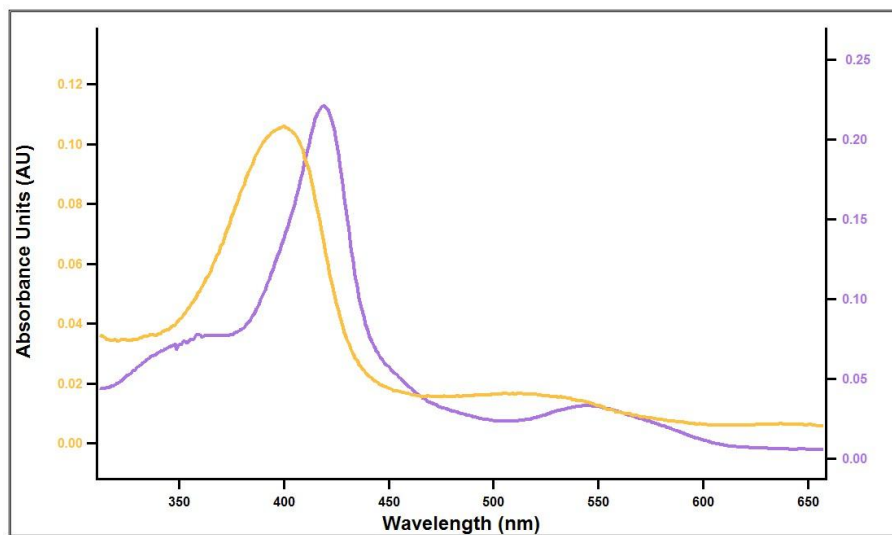
Figure 8: UV-Vis spectroscopy of *Pcc*GCS in the ferric (yellow) and ferric-CN (purple).

Initial Activity

To test whether *Pcc*GCS has diguanylate cyclase activity, *Pcc*GCS was allowed to react with GTP, in the presence of magnesium chloride, at room temperature. Samples were removed at various time points, quenched (EDTA, heat), and precipitated protein removed through centrifugation. The supernatant was then run on a reverse phase C18 column as reported in the experimental section to separate the starting material and products.[15] Using this method, the rate of activity for each ligation state was calculated. As seen in Figures 9 and 10, when oxygen is bound to the globin, the highest initial rate is measured. Oxygen's rate decreases at higher time points since an allosteric product inhibited I-site reduces activity at higher concentrations.[14] This experiment was compelling since not only was *Pcc*GCS found to be active, but oxygen is shown to be the activating ligand. This data supports the hypothesis that oxygen may play a role in biofilm formation by activating *Pcc*GCS.[15] However, the protein in these experiments was purified with some c-di-GMP already bound to the I-site, so these rates are likely slower than the maximal rates for *Pcc*GCS.
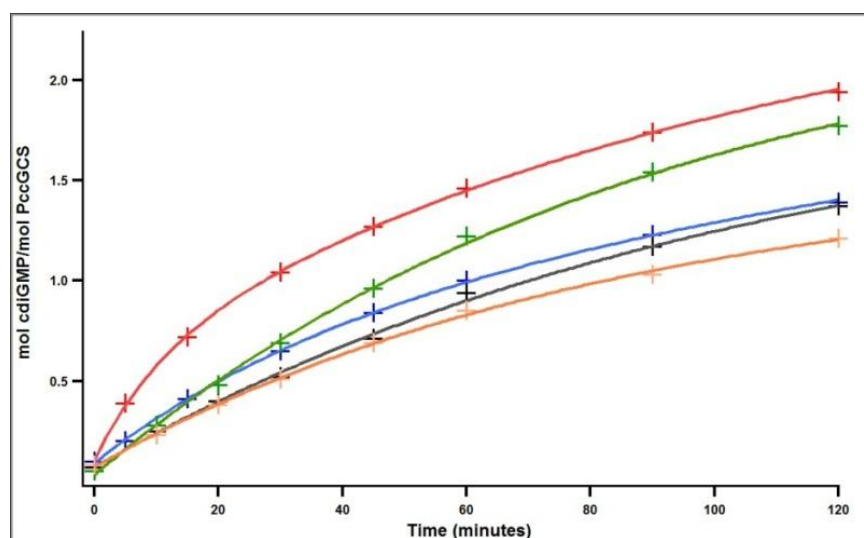
Figure 9: Diguanylate cyclase activity of *Pcc*GCS with differing heme states. FeII-O$_2$ (red), FeII-NO (green), FeII-CO (blue), FeII-unligated (black), and FeIII (orange). Ferrous-oxy displays the highest activity.
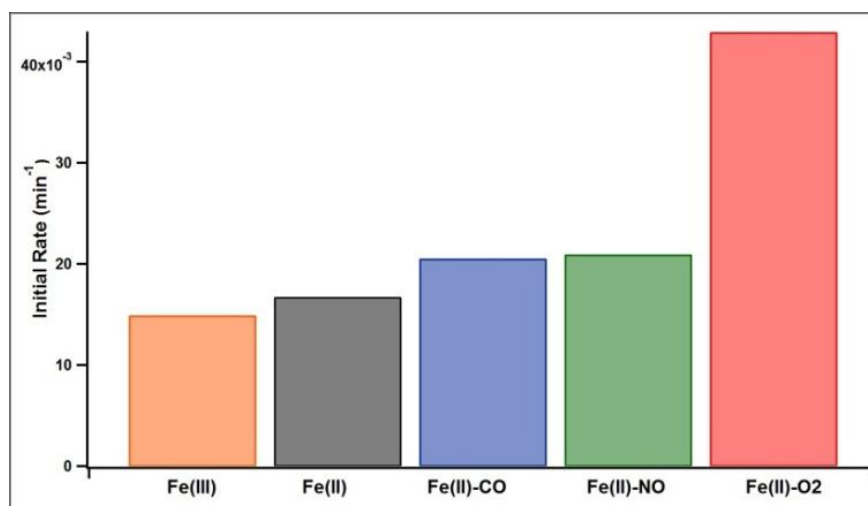
Figure 10: Initial rates of *Pcc*GCS with each heme ligation state: oxygen (red), nitric oxide (green), carbon monoxide (blue), unbound ferrous state (black), and the unbound ferric state (orange).

Optimized Expression

The initial activity most likely represents a slower rate than actually exists for *Pcc*GCS due to partial binding of c-di-GMP in the I-site. *Pcc*GCS has an allosteric inhibitory site that slows down its activity when c-di-GMP is bound.[14] The protein used in the initial activity assay has on average 1.00 ± 0.39 mole c-di-GMP per mole of *Pcc*GCS, indicating that c-di-GMP is inhibiting activity even at the start of the initial experiment. To address the problem of c-di-GMP bound to the I-site, the protein was immediately dialyzed with a phosphodiesterase, D53E HnoB, after expression.[32] The phosphodiesterase hydrolyzes c-di-GMP to the linear pGpG.[33] However, this produced little improvement in the amount of c-di-GMP bound. An optimization of the expression, however, did show significant decrease of bound c-di-GMP. By decreasing the induction time from ~18 hours to six hours, the amount of bound c-di-GMP was lowered to 0.14 ± 0.03 mole c-di-GMP per mole of *Pcc*GCS. During the optimization process, a new cell

line was also used: RP523.[34, 35]   This *E. coli* cell line is permeable to hemin, which allows for direct uptake and use in the expressed protein. Adding hemin directly allows the cell to save energy used in synthesizing the hemin from 5-aminolevulinic acid. RP523 cells also displayed a significant increase in heme incorporation, as seen in Figure 11.
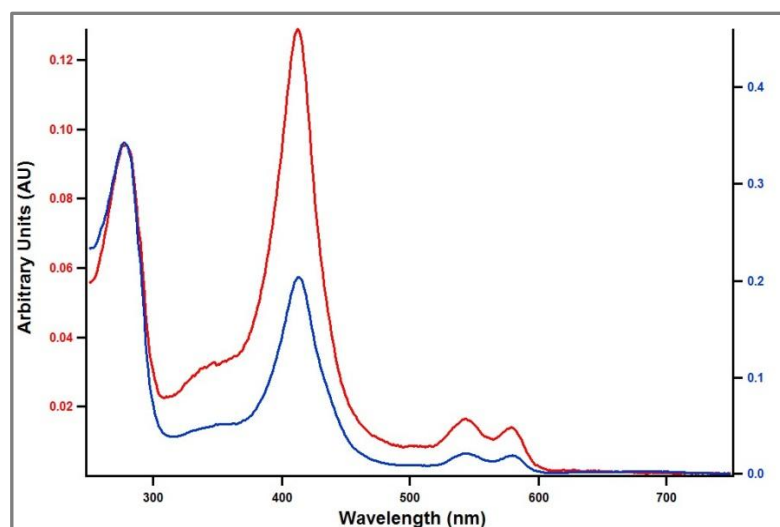
Figure 11: UV-Vis spectra of oxygen bound *Pcc*GCS when expressed in Tuner (DE3) PlysS (blue) and RP523s (red). As seen by the difference in the soret and α-β bands, the heme incorporation is significantly higher in the RP523 expression system.

Enzyme Coupled Assay

In order to limit the allosteric inhibition of c-di-GMP, the activity assay was optimized to run with the phosphodiesterase D53E HnoB.[32]   The activity of the phophodiesterase was measured under similar conditions to the diguanylate cyclase assay (see Methods Section Phosphodiesterase Activity Assay). However, the process of separating D53E HnoB to over 90% purity was found to significantly lower its activity. Therefore, the purification process was optimized to yield the highest activity. The final activity was measured at 6.64 min^{-1}. Optimization improved the rate 190 fold over the

original values; however 6.64 min^{-1} is still significantly lower than the published value of 18 min^{-1}. The activity assay of HnoB is displayed in Figure 12.
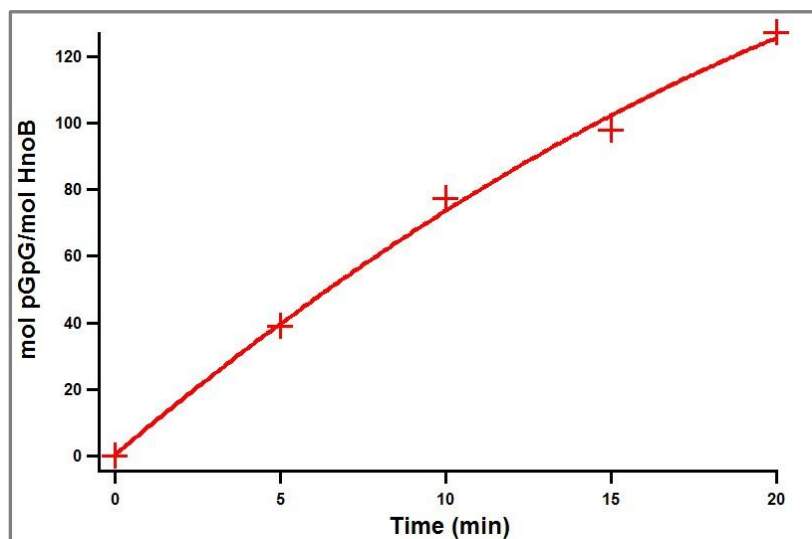
Figure 12: Activity assay of HnoB phosphodiesterase. Measured by mol pGpG per mol HnoB over time. Initial rate is 6.64 min^{-1}.

Since measured HnoB activity was less active than the reported value, another phosphodiesterase, *Ec*DosP, was tested. *Ec*DosP is a phosphodiesterase from *E. coli* with an N-terminal heme-PAS domain.[36] *Ec*DosP was expressed and purified as previously described (see Methods Section *Ec*DosP Purification).[37] An initial activity assay was measured under the same conditions as that of HnoB.   The activity was calculated to be 33.58 min^{-1}, which is significantly faster than the rate (6.64 min^{-1}) measured for HnoB. The initial EcDosP activity assay can be seen in Figure 13.

To measure the non-product inhibited *Pcc*GCS reaction rate HnoB was added at 10x or *Ec*DosP was added at 5x the molar concentration of *Pcc*GCS. The rates of the coupled assay were significantly higher without the presence of c-di-GMP. Switching to a short induction of *Pcc*GCS and adding an active phosphodiesterase to the assay yielded

rates ranging from 0.411 ± 0.09 min^{-1} to 2.48 ± 0.11 min^{-1}. The rate of 2.48 ± 0.11 min^{-1} was measured with active HnoB, is 62 times larger than the observed initial activity, and is very close to the published rate of oxygen bound *Bpe*Greg of 2.5 min^{-1}.[15] However, even the rate of 0.411 ± 0.09 min^{-1} is still 10 times larger than the observed initial activity. The lower rate was measured with either inactive HnoB or active *Ec*DosP. The slower rate coupled with inactive HnoB can be explained by the incomplete conversion of c-di-GMP to pGpG; however, since *Ec*DosP displayed full conversion, it is difficult to rule out this data. Therefore, further analysis is required to distinguish the correct rate. The enzyme coupled assay, run in triplicate, with a rate of 2.48 ± 0.11 min^{-1} and measured with active D53E HnoB is displayed in Figure 14. The enzyme coupled assay, run in triplicate, with a rate of 0.411 ± 0.09 min^{-1} and measured with active *Ec*DosP is shown in Figure 15.
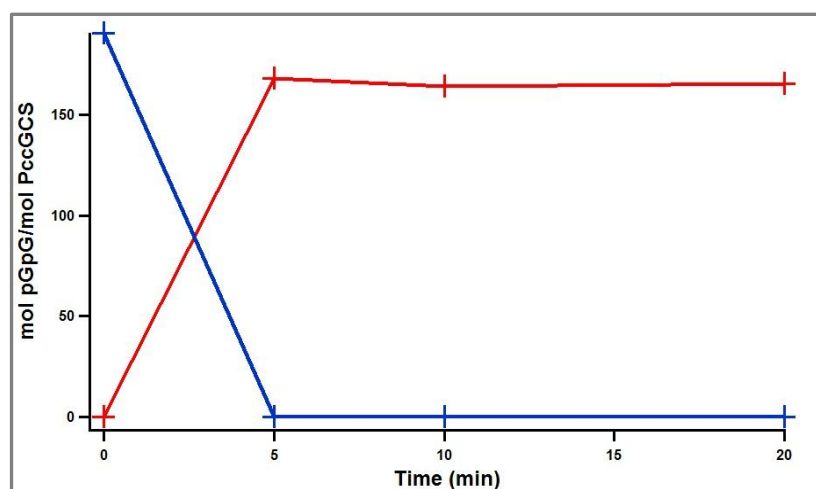
Figure 13: Activity assay of EcDosP. Red line indicates the production of pGpG, and blue line indicates the loss of c-di-GMP. Substrate is immediately consumed, and the initial rate is 33.58 min^{-1}.

Optimization of a non-enzymatic fluorescent pyrophosphate sensor, PhosphoWorks kit (AAT Bioquest), was utilized as previously described by the Boon group.[38] However, after analysis of the assay it was determined that heme significantly quenches reporter fluorescence. Therefore, the EnzCheck assay (Molecular Probes) was utilized to confirm HPLC results. The EnzCheck assay spectroscopically measures phosphate by utilizing purine nucleoside phosphorylase (PNP) to convert 2-amino-6-mercapto-7-methylpurine ribonucleoside (MESG; absorbance maximum of 330 nm) and phosphate into ribose 1-phosphate and 2-amino-6-mercapto-7-methylpurine (absorbance maximum of 360 nm).[39] The kit also includes inorganic pyrophosphatase, which converts pyrophosphate to two individual phosphate molecules. Since four phosphates are created for every synthesis of c-di-GMP, the EnzCheck assay is very sensitive to each conversion. An EnzCheck assay run with mostly inactive D54E HnoB is shown in Figure 16.
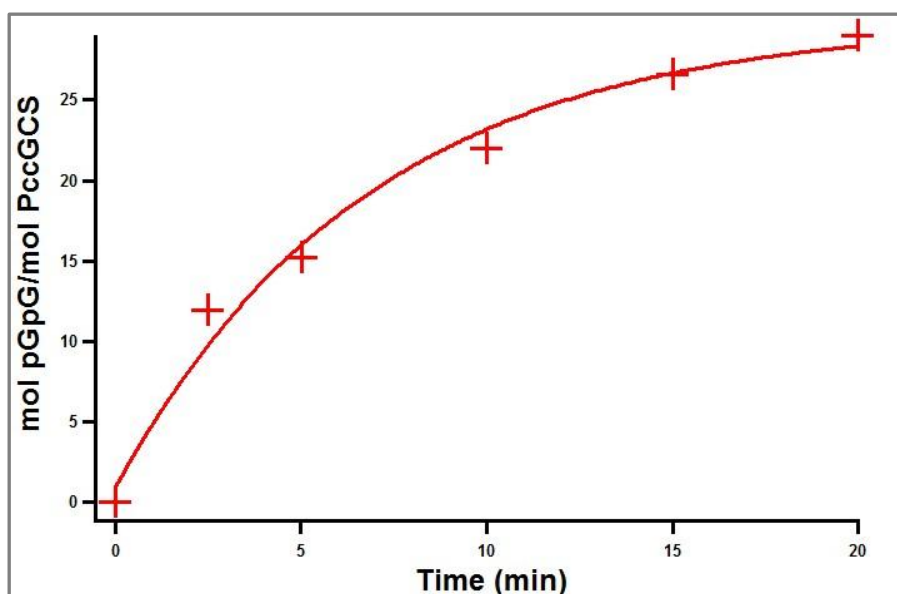
Figure 14: Activity assay of *Pcc*GCS run in triplicate with 10x molar concentration of optimized HnoB. Red line indicates the production of pGpG. Rate of PccGCS for this assay was measured at 2.48 ± 0.11 min^{-1}.
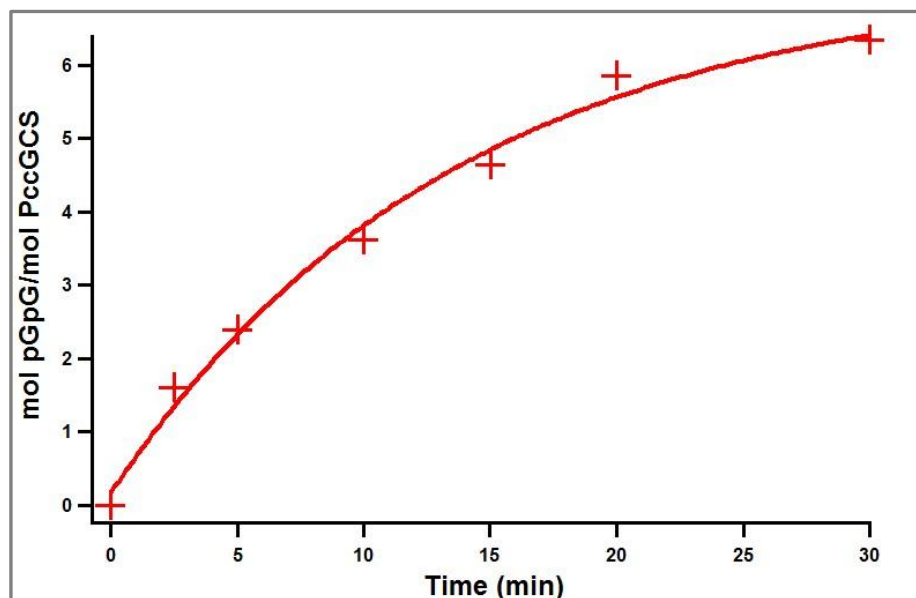
Figure 15: Activity assay of *Pcc*GCS run in triplicate with 5x molar concentration of EcDosP. Red line indicates the production of pGpG. Rate of PccGCS for this assay was measured at 0.479 min^{-1}.
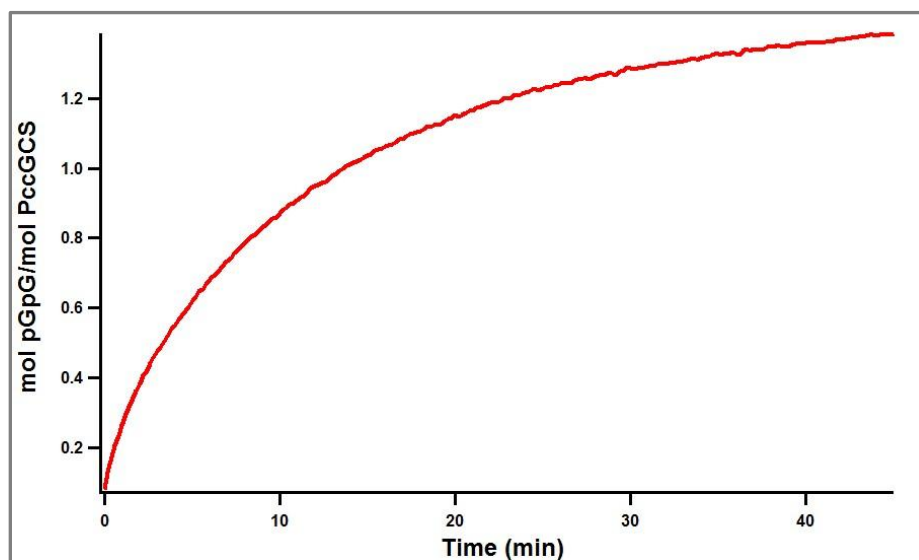
Figure 16: EnzCheck activity assay of *Pcc*GCS with 10x molar concentration of initial HnoB. Red line indicates the production of pGpG. Rate of PccGCS for this assay was measured at 0.415 min^{-1}.

The expression, purification, UV-Vis measurements, and activity assays demonstrate that *Pcc*GCS is an active globin coupled sensor with diguanylate cyclase activity. The heme domain characteristically binds each ligand as well as selectively regulates its diguanylate cyclase output. The activity with each ligand bound was originally measured with c-di-GMP inhibition; however the rate of the oxygen bound *Pcc*GCS was still twice that of the unligated form. The uninhibited activity of oxygen bound *Pcc*GCS was subsequently measured and determined to be within the range of 0.411 ± 0.09 min^{-1} and 2.48 ± 0.11 min^{-1}, which is $10 - 62$ times more active than the c-di-GMP inhibited rate. Since oxygen activates the diguanylate cyclase over other diatomic gases, *Pcc*GCS may have an influence on biofilm formation.[15] With oxygen bound, *Pcc*GCS would be more active, and this active state would allow more c-di-GMP to be produced. Because c-di-GMP concentration is positively associated with biofilm formation, the oxygen activated *Pcc*GCS may be able to induce this less virulent state.[11]

Regulation of Activity through Oligomerization

Since *Pcc*GCS is an active globin coupled sensor with diguanylate cyclase activity, it is beneficial to understand the mechanism by which the globin domain regulates its own diguanylate cyclase. As previous work on PleD and WspR suggests that dimerization is required for activity, oligomerization may have a significant role in regulating numerous globin coupled sensors.[28, 31] Therefore, elucidating the mechanism of *Pcc*GCS communication will not only prove beneficial for *P. carotovorum* but may also provide insight for many other virulent bacteria. The oligomerization states of *Pcc*GCS was tested by Native PAGE gel analysis and analytical gel filtration.

Native PAGE Gel Analysis

Native PAGE gel analysis was optimized for determining the oligomerization states of *Pcc*GCS. Six percent separating solution with either coomassie, silver stain (Pierce), or heme stain[40] resulted in optimal separation of four bands. The four bands most likely correlate with aggregate, octamer, tetramer, and dimer; however due to smearing of the molecular weight standards, the molecular weight of each band was difficult to verify. Gel images are displayed in Figure 17. Though Native gels containing a significant concentration of sodium dithionite could be conducted to determine the oligomerization of the ferrous-unligated state within the heme, anaerobic conditions may be difficult to simulate. Therefore, the native PAGE gels were useful in discovering that *Pcc*GCS forms higher order oligomers, but AGF analysis was further pursued since the native gels do not provide quantitative evidence.
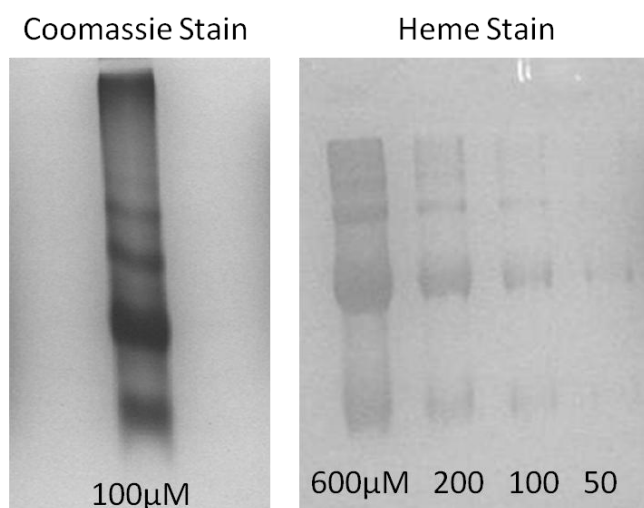
Figure 17: Native PAGE gel of oxygen bound *Pcc*GCS. All display four bands, most likely correlating to aggregate, octamer, tetramer, and dimer states.

Distributions of Oxygen Bound and Unligated Heme States

Oxygen bound, ferrous-unligated, ferrous-CO, and ferric heme were found to consist of differing percentages of homo-octamer, tetramer, and dimer. Since proteins can change oligomeric state in response to varying concentrations, the correlation of oligomer formation with increasing protein concentration was first explored with analytical gel filtration. As seen in Figure 18, the percentage of oligomer is not dependent on protein concentration. Therefore, other methods of oligomeric regulation were pursued.
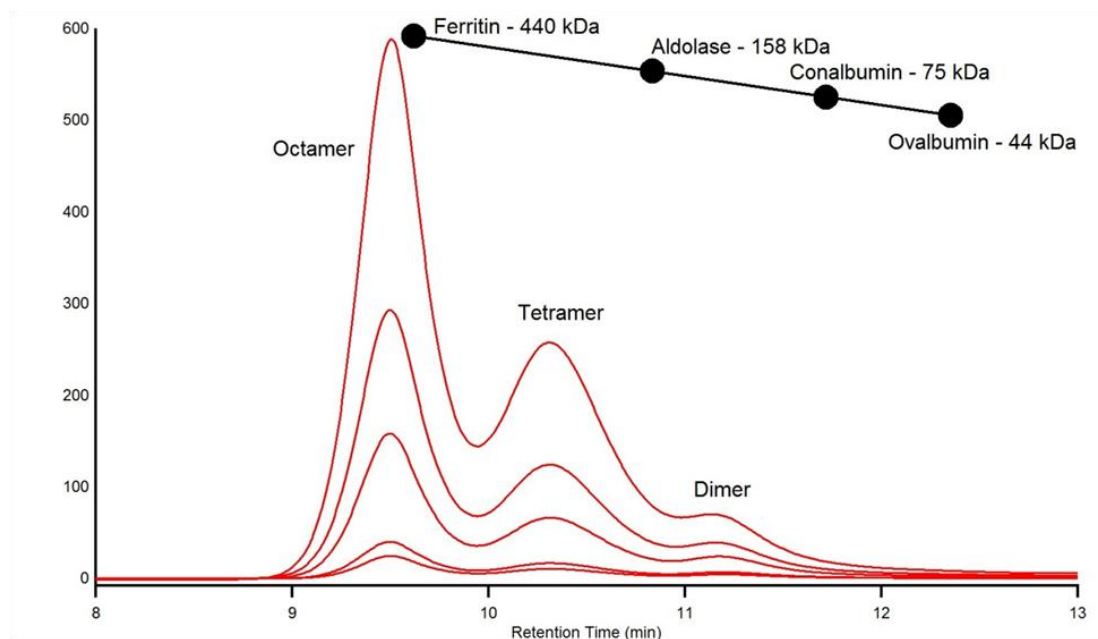
Figure 18: AGF trace at 214 nm of ferrous-oxy *Pcc*GCS at 2.5 µM, 5 µM, 12.5 µM, 50 µM, and 100 µM PccGCS. High molecular weight standards are displayed on top of the trace.

A small shift from tetramer to dimer is observed when comparing oxygen bound heme with the ferrous-unligated state, as seen in Figure 19. This shift suggests that oxygen binding may lead to dimer formation. However, the error bars make the shift statistically insignificant. Since this data was acquired before the optimized expression of *Pcc*GCS, high error bars may be due to the varying concentrations of c-di-GMP bound to the protein sample. On another note, each HPLC run can display the full UV-Vis spectrum at every time point. Therefore, the ligand that is bound to the heme can be experimentally confirmed. This is especially useful in confirming the unligated state of the heme. When viewing the peaks from the unligated AGF runs, there is a dominant soret band at 433 and one alpha beta band. This signature UV-Vis spectra indicates that the heme is unligated. Optimization of differing concentrations of dithionite in the buffer

as well as an alteration of the column flushing times was conducted.[41] A comparison of the full spectra from the octamer peak is shown in Figure 20.
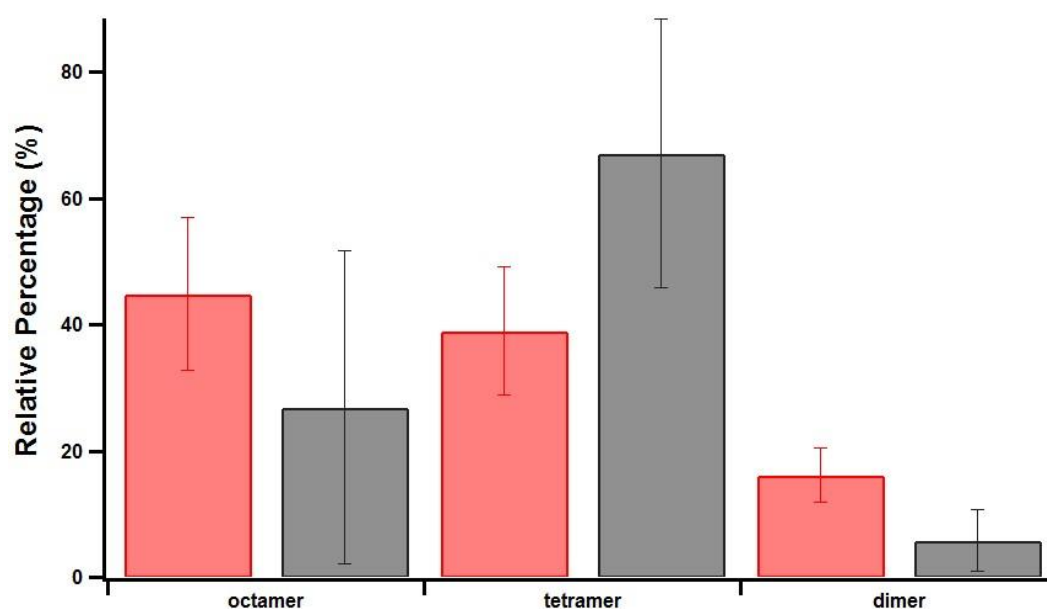
Figure 19: Relative percentages of ferrous-oxy (red) and ferrous –
unligated (gray) heme at 214 nm. Triplicate experiments.

The percentage of octamer was also observed to vary considerably between protein samples from different purifications. Therefore, two possible explanations were devised. Firstly, since the *Pcc*GCS was purified with a 6x His tag, it may be possibly that the histidine residues are affecting oligomerization. Secondly, since previous literature on WspR oligomerization and experiments detailed above found that diguanylate cyclase domains can purify with c-di-GMP bound to the I-site which alters diguanylate cyclase oligomerization,[29] it seems likely that octamer formation may change based on the concentration of c-di-GMP bound. Therefore, both options were further explored.
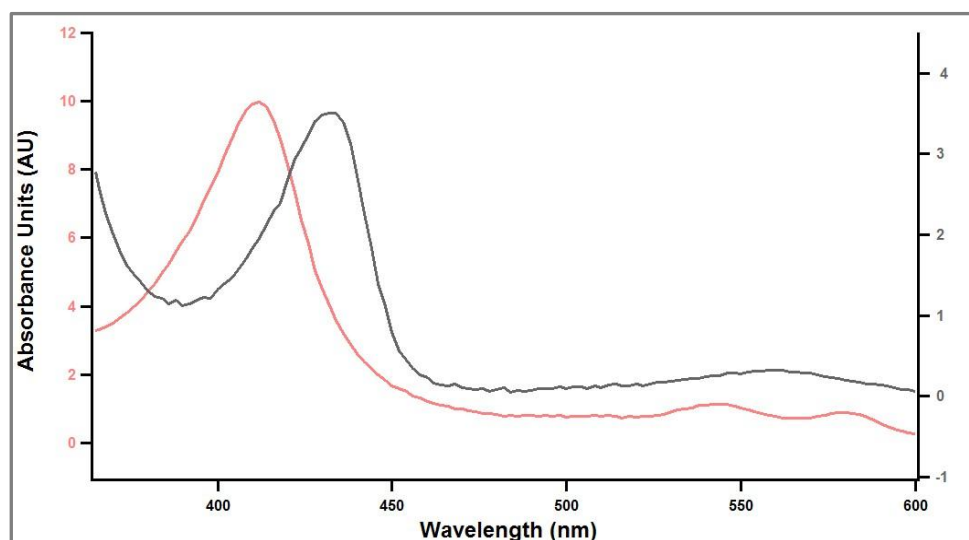
Figure 20: Full spectra comparison of the octamer peak between ferrous-oxy (red) and ferrous-unligated (gray) *Pcc*GCS. The ferrous-unligated soret at 433 and single alpha beta band indicates that the heme is still unligated.

Role of the His tag

After initial runs of ferrous-oxy and ferrous-unligated *Pcc*GCS, the octamer peak was further analyzed in order to determine whether the His tag plays a role in forming high level oligomerization states. Since His tags binds to metal, it is possible that the higher order oligomers were caused by the His-tags chelating metal in solution. Therefore, equal and 5x concentration of nickel was added to protein samples and the mixture run on AGF. The percentages of octamer remained consistent between samples with and without added nickel. Factor Xa was also used to cleave the His tag from the protein sequence.[42] However, this scareless cleavage procedure produced a significant amount of protein precipitation after incubation with Factor Xa removal resin, making it difficult to draw a conclusion from this data. Following cleavage, the soluble protein was run and displayed a larger octamer peak than measured with a His tag. Based on these

experiments, the His-tag does not seem to play a large role in octamer formation, but further studies may be required. Simultaneously, the variation of relative octamer percentages based on the concentration of c-di-GMP bound to *Pcc*GCS was further explored and yielded more conclusive data.

Distributions of R364A *Bpe*Greg

Many diguanylate cyclases have a product-binding allosteric site that inhibits catalytic activity. When c-di-GMP binds to *PccGCS*'s allosteric site, characterized by an RXXD motif, further cyclization of GTP is inhibited.[43] While measuring the relative percentages of oligomers, a change in octamer composition was observed between separate expressions. Therefore, the effect of c-di-GMP bound to the I-site was measured through an I-site defective variant.
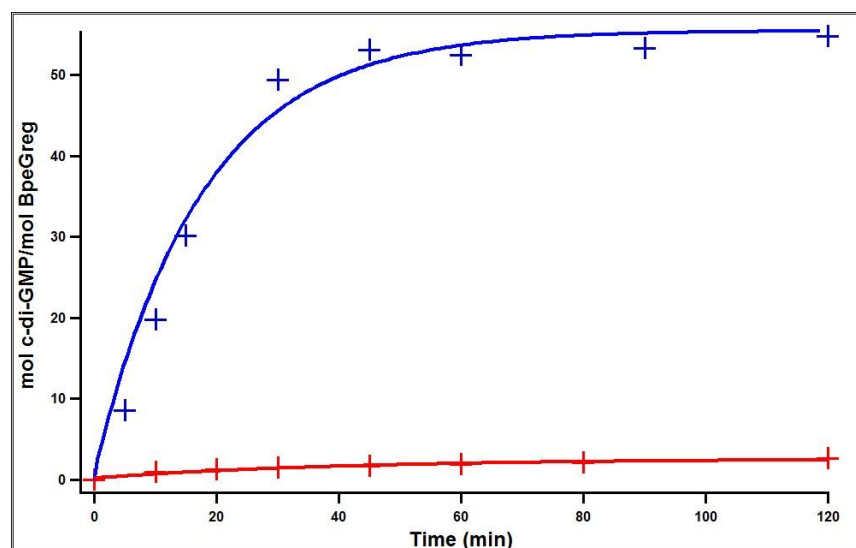
Figure 21: Activity assay of R364A *Bpe*Greg (blue) and c-di-GMP inhibited *Bpe*Greg (red). R364A BpeGreg has an initial rate of 2.03 min^{-1}, which is 44 times larger than the inhibited BpeGreg rate of 0.046 min^{-1}.

In 2009, Rao designed a thermophilic diguanylate cyclase variant that could not bind c-di-GMP by changing the conserved arginine to an alanine.[44] This variant allows for uninhibited formation of c-di-GMP. Site-directed mutagenesis was utilized to alter *Bpe*Greg, a homologous globin coupled sensor from *B. pertussis* that is also studied within the laboratory. The R364A variant of *Bpe*Greg was expressed and tested for activity by the previously described HPLC method (see Methods Sections R364A Purification and DGC Activity).[15] As seen in Figure 21, the activity is significantly higher at 2.03 min^{-1} than the inhibited wild type rate of 0.046 min^{-1} measured in the lab, the reported uninhibited rate for wild type *Bpe*GReg is 2.5 min^{-1}. As these rates are very similar, it is unlikely that the R364A mutation affected catalysis.
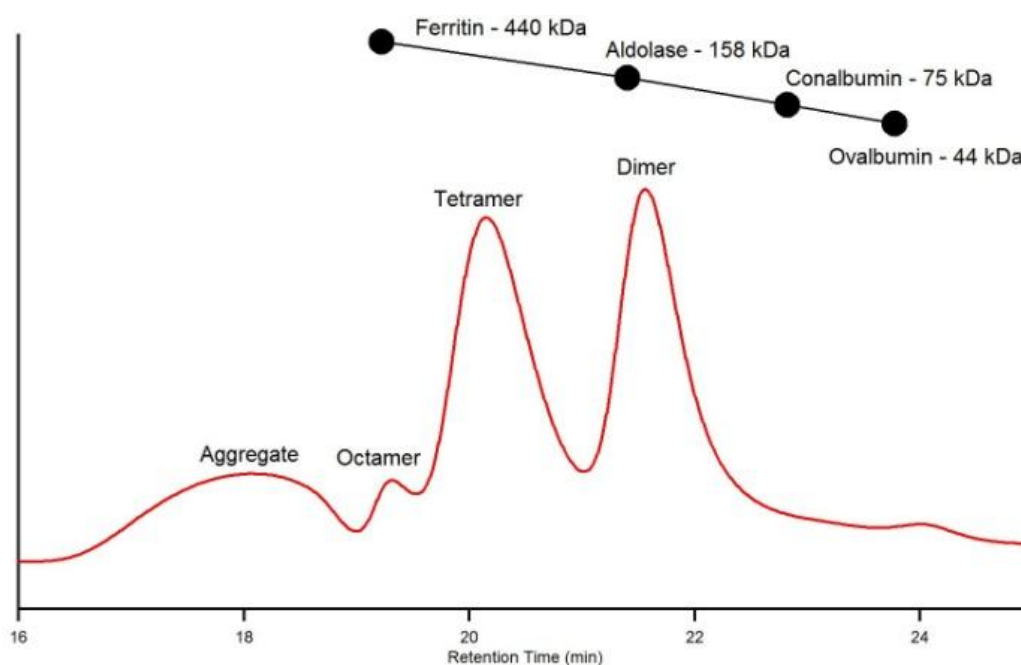
Figure 22: AGF trace of ferrous-oxy R364A *Bpe*Greg; high molecular weight standards are displayed on top of the trace.

The R364A mutant's oligomerization properties were also measured with analytical gel filtration. Preliminary AGF data of oxygen bound R364A *Bpe*Greg displays a significant decrease in octamer formation, shown in Figure 22. This suggests that the I-site of this globin coupled sensor may play a regulatory role by inducing octamer formation.

After oxygen was determined to activate the catalytic domain of *Pcc*GCS, the mechanism of oligomeric regulation was explored. Native PAGE gel analysis first showed that *Pcc*GCS produces four high order states. However since the gels did not yield quantitative data, analytical gel filtration was utilized. Surprisingly, AGF studies revealed no correlation between protein concentration and high order states. Instead, a small shift toward dimer was observed when oxygen was present, suggesting that the binding of oxygen may induce a catalytically active homodimeric state. Since the error bars made this shift statistically insignificant, the cause of variation within the runs was further analyzed. C-di-GMP binding and relative octamer percentages were both found to vary between protein purifications. Therefore the R364A *Bpe*Greg I-site variant, that cannot bind c-di-GMP, was analyzed and shown to have significantly less octamer than the wild type protein. This data suggests that c-di-GMP may inhibit activity through association of an inactive octamer. Though further studies are necessary to verify the precise oligomeric regulation, this is the first study to propose a mechanism for the communication between the sensing globin and catalytic output domains of globin coupled sensors with diguanylate cyclase activity.

Conclusion and Future Directions

Given the widespread damage of *P. carotovorum* infection, ongoing research is necessary to develop new improvements in soft rot containment. This study investigates the role of globin coupled sensors in *P. carotovorum* biofilm formation and virulence. Since spread of *P. carotovorum* is highly dependent on oxygen concentration,[5, 6] it was hypothesized that *Pcc*GCS plays a role in virulence through an oxygen dependent initiation of a sessile state. Therefore *Pcc*GCS was tested *in vitro* and discovered to be activated by oxygen, suggesting that this hypothesis may be true. Further studies of *Pcc*GCS oligomerization suggest that oxygen binding at the heme induces an active homodimer and that ferrous-unligated heme shifts the equilibrium toward an inactive tetramer. Preliminary data also shows that binding of c-di-GMP at an allosteric inhibitory site may induce a hyper-inactive octamer. These findings yield an improved understanding of *Pcc*GCS as an active globin coupled sensor within *P. carotovorum*.

The initial expression, purification, UV-Vis measurements, and activity assays demonstrate that *Pcc*GCS is an active globin coupled sensor with diguanylate cyclase activity. However, self-inhibition inherent in the initial assay was found to affect the measured rates. Though the activity of the globin coupled sensor was initially inhibited, the oxygen bound *Pcc*GCS still yielded a rate twice that of the unligated form. This data indicates that oxygen, as in other homologous proteins, may be the activating ligand of *Pcc*GCS.[15, 22, 24] In order to modify the activity assay, two phosphodiesterases were expressed, tested for activity, and coupled to the *Pcc*GCS assay.[32, 37] The optimized rate is determined to be within $0.411 - 2.48$ min^{-1}, which is $10 - 62$ times larger than the observed initial activity. Though further studies would need to be conducted to

determine the rate difference between the uninhibited oxygen and unligated heme states, these experiments indicate that oxygen activates the diguanylate cyclase over other diatomic gases, suggesting that *Pcc*GCS may have an influence on biofilm formation.[15]

Once *Pcc*GCS was determined to be an oxygen activated globin coupled sensor, the mechanism of signal transmission through oligomerization was tested using analytical gel filtration. Though it was initially thought that *Pcc*GCS oligomerization would be concentration dependent, a correlation between protein concentration and oligomerization was not found. Therefore, other mechanisms of oligomeric control were explored. When comparing the oxygen bound and unligated states, a small shift between the relative percent of dimer and tetramer was discovered. Though deviations between protein preparations make the error bars too large for statistical analysis, the shift indicates that the oxygen bound state may initiate dimer formation. Since large differences in the octamer peak varied significantly between preps in correlation with the amount of c-di-GMP bound, an I-site inactive variant of *Bpe*Greg, a globin coupled sensor simultaneously studied in the lab, was tested by analytical gel filtration.[15, 44] The octamer peak of R364A *Bpe*Greg was significantly decreased, indicating that c-di-GMP may have a role in octamer formation.

This study reveals an overall understanding of the activity and mechanism of *Pcc*GCS. However, further studies would be beneficial. Utilization of the optimized enzyme coupled activity assay could be used to determine the precise increase of *Pcc*GCS activity between the uninhibited oxygen bound and unligated states. Also, c-di-GMP was successfully added back to the c-di-GMP free *Pcc*GCS protein stock (1.04 ± 0.11 mol c-di-GMP / mol *Pcc*GCS). Directly comparing the c-di-GMP free and c-di-

GMP bound *Pcc*GCS on analytical gel filtration would develop a more thorough picture of *Pcc*GCS's mechanism. Finally, *in vivo* studies would be beneficial in determining *Pcc*GCS's direct role in oxygen sensitive biofilm formation.

In vivo analysis of *Pcc*GCS would directly correlate *P. carotovorum*'s oxygen-dependent virulence with the activation of a diguanylate cyclase. The gene coding for *Pcc*GCS in *P. carotovorum* is currently being deleted through allelic exchange by a post-doctoral researcher.[45] The Δ*Pcc*GCS strain could be used to compare biofilm formation in aerobic and anaerobic environments with a crystal violet assay.[46] Once created, the *P. carotovorum* Δ*Pcc*GCS strain is predicted to reduce oxygen sensitivity of biofilm formation. After testing *P. carotovorum's* ability to form biofilms in a range of oxygen concentrations, *Pcc*GCS's role in virulence could be analyzed through the inoculation of potato tubers with *P. carotovorum*.[7] The Δ*Pcc*GCS strain is hypothesized to be more virulent compared to wild type. These experiments will test whether *Pcc*GCS senses oxygen levels and consequently regulates the switch between motile and sessile states *in vivo*.

Bacteria have adopted intricate mechanisms in order to sense and respond to their environment. This study begins to paint a picture of the role of *Pcc*GCS in sensing surrounding oxygen concentrations and responding to its environment by forming less-virulent biofilms. It is beneficial for the bacteria to form biofilms since many plants require oxygen for structurally sound cell membranes and contain oxygen-dependent defenses against bacteria.[3] Therefore in the anaerobic state, *P. carotovorum* has a higher chance of survival and can use extra resources for growth and virulence. This study links *Pcc*GCS to *P. carotovorum*'s lower virulence in an aerobic state. Since *Pcc*GCS is

activated by oxygen, more c-di-GMP is produced when oxygen is present which should lead to biofilm formation.[11] Further studies of *Pcc*GCS oligomerization suggest that oxygen binding at the heme induces an active homodimer and that binding of c-di-GMP at an allosteric inhibitory site may induce a hyper-inactive octamer. Understanding bacterial defense mechanisms will prove beneficial in designing new targets for the artificial formation or dispersion of biofilms. These findings yield an improved picture of the overall globin coupled sensor mechanism and lead to a better understanding of oxygen's role in biofilm regulation of *P. carotovorum*.

Experimental Methods

Sequence Alignment and Homology Modeling of *Pcc*GCS

The sequence alignment of EcDos and BpeGreg (two published globin coupled sensors) with the sensors in *P. carotovorum*, *D. dadantii* was accomplished with Clustal X.

The homology model of a globin coupled sensor was based on the PDBs 1OR4 and 3BRE.

Site-Directed Mutagenesis

Site directed mutant R364A *Bpe*Greg was created with mutagenic primers:

FP: 5' –GATTGCTAGTTATTCCCGTGGCGGTGATTACACC – 3'

RP: 5' – GGTGTAATCACCGCCACGGGAATAACTAGCAATC – 3'

PCR was performed with *Phusion* polymerase (New England Biolabs) and run according to manufacturers' conditions. DpnI (New England Biolabs) was added to 4% of the total volume and incubated for 2 hours at 37ºC. PCR solutions were immediately transformed into DH5α (New England Biolabs).

*Pcc*GCS, *Bpe*Greg, HnoB, and *Ec*DosP Expression

Proteins were expressed in Tuner (DE3) PlysS cells or RP523 cells (*Pcc*GCS only).

Tuner Expression:

Overnight cultures of Tuner (DE3) PlysS cells previously transformed with respective plasmid were made with 10 mg/ml Ampicillin and 3 mg/ml chloramphenicol (Research Products International Corp.). 20 mL of an overnight culture was added to 45g bacto-yeast extract (Research Products International Corp.), 1.6 g of KH_2PO_4, 11.5 g of $K_2HPO_4 \cdot 3H_2O$, 10-15mL glycerol (Sigma-Aldrich), and 1 L of milli-q water. Flasks were grown at 37ºC until an OD of 0.8 - 1.0. The cultures were then induced with 500 µM 5-aminolevulinic acid (OChem, Inc.), 100 µM isopropyl-β-D-thiogalactopyranoside (Research Products International Corp.), and 10 µM ferric chloride (Sigma-Aldrich) at 18ºC. The cultures were incubated at 18ºC for 18 - 20 hours. Cultures were then harvested by centrifugation at 6,000 rpm for 15 minutes and stored at -80C.

RP523 Expression:

Overnight cultures of RP523 cells previously transformed with respective plasmid were made with 10 mg/ml Ampicillin (Research Products International Corp.). 20mL of an overnight culture was added to 1L of Terrific Broth (Research Products International Corp.) with 15ug/ml hemin (Frontier Scientific). Flasks were grown at 37ºC until an OD of 0.8 - 1.0. The cultures were then induced with 100 µM isopropyl-β-D-thiogalactopyranoside (Research Products International Corp.) and incubated at 20ºC for 6 hours. Cultures were then harvested by centrifugation at 6,000 rpm for 15 minutes and stored at -80°C. Light was limited where possible to reduce hemin decomposition.[34, 35]

_Pcc_GCS, _Bpe_Greg, HnoB, _Ec_DosP Purification

_Pcc_GCS and R364A _Bpe_Greg Purification:

1 L pellets were thawed on ice with low imidazole buffer (50 mM Tris HCl, 300 mM NaCl, 20 mM Imidazole, 5% glycerol, pH 8), 1 mM pefablock (GoldBio, tech), a pea-sized amount of benzamidine (Research Products International Corp.), and 0.02 mg/mL DnaseI (Calbiochem). The solution was mixed until homogeneous and lysed 3x using an homogenizer (EmulsiFlex-C5). The lysate was centrifuged at 40,000 rpm (Beckman-Coulter) for 60 minutes and the supernatant loaded onto a nickel column previously equilibrated with 10 column volumes of low imidazole buffer. The protein was eluted with a gradient (0-50 mL, 2% B; 50-100 mL, 4% B; 100-150 mL, 7% B; 150-200 mL, 9% B; 200-250 mL, 11% B; 250-300 mL, 13% B; 300-735 mL, 13-100% B) of high imidazole buffer (50 mM Tris HCl, 300 mM NaCl, 5% glycerol, pH 7.5). After which the protein fractions were concentrated (Sartorius Vivaspin; 30K MWCO) and desalted with a PD 10 column (GE Healthcare) into storage buffer (50 mM Tris HCl, 50 mM NaCl, 250 mM Imidazole, 5% glycerol, 1 mM DTT, pH 7.5). If the protein was not adequately purified with solely a nickel column, it was subjected to a gel filtration column (GE Healthcare; HiLoad 26/600) on a medium flow FPLC (Bio-Rad; BioLogic Dual flow). Fractions were concentrated, aliquoted, immediately frozen in liquid nitrogen, and stored at -80ºC. With the exception of homogenization, all purification protocols were performed at 4ºC. An example SDS page gel of _Pcc_GCS is shown in Figure 23.
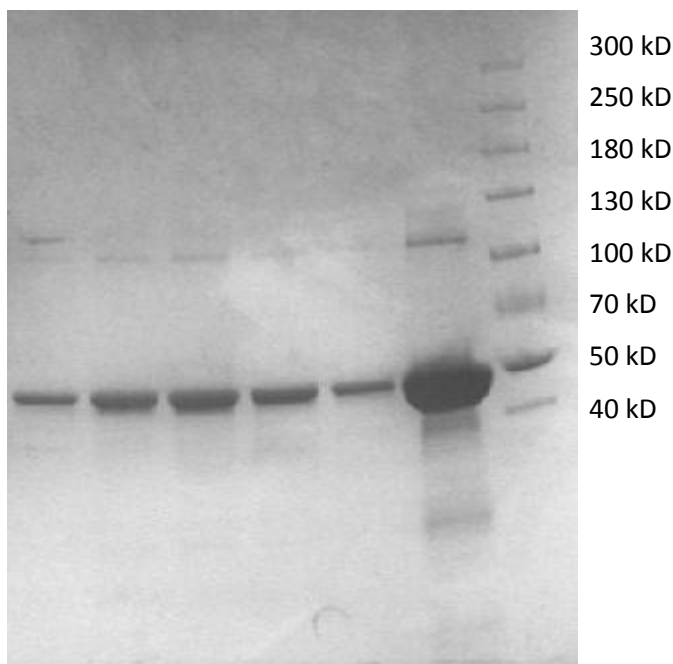
**Figure 23: SDS PAGE gel of *Pcc*GCS, stained with Coomassie blue. First 5 lanes
consist of fractions after gel filtration, and 6th lane is after concentration.
Molecular weight is 54 kD**

HnoB Purification:

1 L pellets were thawed on ice with Tris buffer (50 mM Tris HCl, 300mM NaCl, 5%
glycerol, 2 mM 2-mercaptoethanol, pH 8) with 1 mM pefablock (GoldBio, tech), a pea-
sized amount of benzamidine (Research Products International Corp.), and 0.02 mg/mL
DnaseI (Calbiochem). The solution was mixed until homogeneous and lysed 3x using an
homogenizer (EmulsiFlex-C5). The lysate was centrifuged at 40,000 rpm (Beckman-
Coulter) for 60 minutes and the supernatant loaded onto an amylose column previously
equilibrated with 10 column volumes of Tris buffer. The protein was washed with 20
column volumes of Tris buffer and eluted with 6 column volumes of maltose buffer (50
mM Tris HCl, 300 mM NaCl, 5% glycerol, 50 mM maltose, 2 mM 2-mercaptoethanol,
pH 8). After which the elution was concentrated (Sartorius Vivaspin; 30K MWCO),

aliquots were immediately frozen in liquid nitrogen and stored at -80C. When protein was run through gel filtration column, significant activity was lost. With the exception of homogenization, all purification protocols were performed at 4ºC.[32] An example SDS page gel of HnoB is shown in Figure 24.
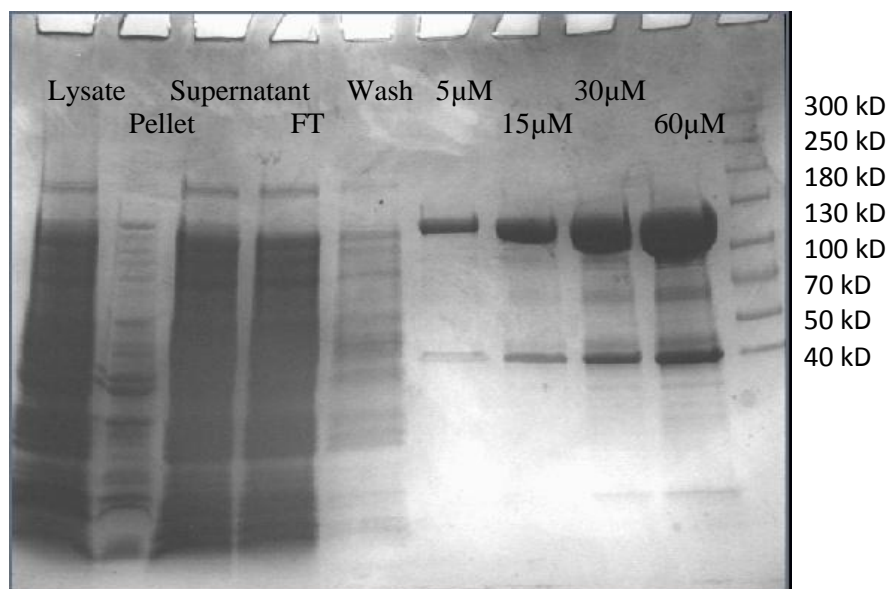
Figure 24: SDS PAGE gel of HnoB with MPB tag (MW 125 kD), stained with Coomassie blue. FT indicates flow through from amylose column.

*Ec*DosP Purification:

1 L pellets were thawed on ice with low imidazole buffer (50 mM Tris HCl, 300 mM NaCl, 20 mM Imidazole, 5% glycerol, pH 8), 1 mM pefablock (GoldBio, tech), a pea-sized amount of benzamidine (Research Products International Corp.), and 0.02 mg/mL DnaseI (Calbiochem). The solution was mixed until homogeneous and lysed 3x using an homogenizer (EmulsiFlex-C5). The lysate was centrifuged at 40,000 rpm (Beckman-Coulter) for 60 minutes and the supernatant loaded onto a nickel column previously equilibrated with 10 column volumes of low imidazole buffer. The protein was washed

with 20 column volumes of low imidazole buffer, and eluted with 5 column volumes of high imidazole buffer (50 mM Tris HCl, 300mM NaCl, 5% glycerol, pH 7.5). After which the protein fractions were concentrated (Sartorius Vivaspin; 30K MWCO) and desalted with a PD 10 column (GE Healthcare) into storage buffer (50 mM Tris HCl, 50mM NaCl, 250 mM Imidazole, 5% glycerol, 1 mM DTT, pH 7.5). Concentrated protein was aliquoted, immediately frozen in liquid nitrogen, and stored at -80ºC. With the exception of homogenization, all purification protocols were performed at 4ºC.[37]

Absorption spectra

Absorption spectra were obtained in storage buffer. Each ligation state is typically prepared by adding excess potassium hexacyanoferrate(III) (Sigma-Aldrich) for oxidation of the heme and sodium dithionite (Acros Organics) for the reduction of the heme. However, precipitation and non-uniform readings were obtained from this process. Therefore, the *Pcc*GCS and *Bpe*Greg reduction process was altered so that only reductant was added to the heme. The ferric state was detected by UV-Vis spectroscopy (Carey) with a signature soret absorbance of 390-415, which corresponds to a mixture of 5- and 6-coordinate states. The ferrous-unligated state was produced by adding excess sodium dithionite, which is identified by a soret maxima at 431 nm with one peak in the alpha-beta band region at 550 nm. By exposing ferrous-unligated heme to oxygenated buffer, ferrous-oxy was formed and identified with a soret at 416 nm and a two peak alpha-beta region. Flushing the ferrous-unligated sample with carbon monoxide yields ferrous-CO bound heme which has a distinctive 422 nm soret, and adding nitric oxide to ferrous-unligated produces ferrous-NO with a 420 nm soret.[15]

Initial and R364A *Bpe*Greg DGC Assay

Enzymatic reactions were conducted with 5 µM protein in storage buffer containing 100 mM $MgCl_2$, performed at room temperature, and initiated with 500 µM GTP. Time points were quenched by removing 50 µl aliquots and heating for 10 min at 90ºC. The samples were centrifuged for 15 minutes at 14,000 rpm, and 20 µL of the supernatant was injected on an Infinity 1260 HPLC system (Agilent Technologies, Germany) with an attached C18 (Agilent Microsorb-MW; 250·4.6 mm) and guard column (Agilent MetaGuard Pursuit, 5u, 4.6 mm). A linear gradient from 0% to 35% B for 10 min at 1 ml/min was conducted (Buffer A: 150 mM sodium phosphate; Buffer B: buffer A with 40% acetonitrile).[15] Standard concentrations of pGpG and c-di-GMP (BioLogic) were run for molar quantification. Anaerobic activity assays were conducted in a glove bag (Coy lab products), and protein concentration was measured by a Bradford Assay (Peirce Scientific).

Phosphodiesterase Activity Assay

Optimized Enzymatic reactions were conducted with 2.5 µM protein in Tris storage buffer containing 10 mM $MgCl_2$, performed at room temperature, and initiated with 500 µM c-di-GMP.[32] Time points were quenched by the same method as described in 'Initial DGC activity'. Standard concentrations of pGpG and c-di-GMP (BioLogic) were run for molar quantification.

Enzyme Coupled DGC Assay

Enzymatic reactions were conducted with 2.5 µM enzyme. Enzyme coupled assays had either 10-fold molar excess of HnoB or 5-fold molar excess of *Ec*DosP. Reactions were conducted in Tris storage buffer containing 100 mM $MgCl_2$, performed at room temperature, and initiated with 500 µM GTP.[15] Time points were quenched by the same method as described in 'Initial DGC activity'. Standard concentrations of pGpG and c-di-GMP (BioLogic) were run for molar quantification.

.

Analytical Gel Filtration

Oligomerization state of *Pcc*GCS was tested by analytical gel filtration (column: Agilent Bio SEC-3, 3 µM particle size) on an Infinity 1260 HPLC system (Agilent Technologies, Germany). After optimization, running conditions consist of a 0.2 ml/min flow rate of 150 mM Phosphate, pH 7 running buffer and 2 µL injection volume. Anaerobic conditions also contain 500µM sodium dithionite in the running buffer.[41] High molecular weight standards (GE Healthcare) were also run after each experiment.

Factor Xa Cleavage

Overnight reaction of Factor Xa cleavage reaction was made with 1 mg of *Pcc*GCS per 10 Units of Factor Xa (Novagen) and diluted with 10x cleavage buffer (1M NaCl, 500mM Tris, pH 8). Reaction sat overnight at room temperature.[42] Factor Xa was subsequently removed with Xarrest removal resin, and further purified by keeping the flow through from a nickel column pre-equilibrated with 10x cleavage buffer.

Adding Back c-di-GMP

PD 10 desalting columns (GE Healthcare) were equilibrated with c-di-GMP buffer 5mM Na2HPO4, 5 mM KCl, 10 mM MgCl2, 1 mM DTT, pH 7.4, 5% glycerol buffer.[47] *Pcc*GCS was desalted into c-di-GMP buffer and sat 18 hours at 4ºC with 2x molar excess of c-di-GMP. The protein was desalted after overnight incubation. C-di-GMP concentration was measured by heating the sample for 10 min at 90ºC, centrifuging for 15 minutes at 14,000 rpm, and injecting 20 µL of the supernatant on an Infinity 1260 HPLC system (Agilent Technologies, Germany) with an attached C18 (Agilent Microsorb-MW; 250·4.6 mm) and guard column (Agilent MetaGuard Pursuit, 5u, 4.6 mm). The protein concentration was measured by Bradford assay (Peirce scientific). The c-di-GMP buffer proved most efficient compared to various concentrations of either Hepes or Tris buffer.

Native Page Gel

6% Tris-glycine native page gel was optimized for best separation. Native page gels were run at 30 mA for 1 hour with Native gel running buffer (0.192M glycine, 0.25 M Tris pH 8.5) and stained with either coomassie blue, silver stain (Peirce scientific), or heme stain. Heme staining consisted of washing the gel for 10 min with 50mL of MeOH/0.25M sodium acetate, pH 5; washing for 20 min in dark with 6 mM DMB in MeOH/0.25M sodium acetate, pH 5; developing for 60 min in dark by adding 235 µL 30% hydrogen peroxide (stored in 4°C); washing for 30 min in H2O/MeOH/acetic acid; and imaged.[40, 48]

References

1.   Toth, I. K.; Birch, P. R., Rotting softly and stealthily. *Current opinion in plant biology* **2005,** *8* (4), 424-9.

2.   Barras, F.; van Gijsegem, F.; Chatterjee, A. K., Extracellular Enzymes and Pathogenesis of Soft-Rot Erwinia. *Annual Review of Phytopathology* **1994,** *32* (1), 201-234.

3.   Toth, I. K.; Bell, K. S.; Holeva, M. C.; Birch, P. R., Soft rot erwiniae: from genes to genomes. *Molecular plant pathology* **2003,** *4* (1), 17-30.

4.   Pérombelon, M. C. M., Potato diseases caused by soft rot erwinias: an overview of pathogenesis. *Plant Pathology* **2002,** *51* (1), 1-12.

5.   Butler, W.; Cook, L.; Vayda, M. E., Hypoxic stress inhibits multiple aspects of the potato tuber wound response. *Plant physiology* **1990,** *93* (1), 264-70.

6.   Vayda, M. E.; Schaeffer, H. J., Hypoxic stress inhibits the appearance of wound-response proteins in potato tubers. *Plant physiology* **1988,** *88* (3), 805-9.

7.   Kelman, S., Influence of oxygen concentration and storage factors on susceptibility of potato tubers to bacterial soft rot (Erwinia carotovora). *Potato Res.* **1978,** *21*, 15.

8.   Lund, B.M., The effect of oxygen and carbon dioxide concentrations on bacterial soft rot of potatoes. *Potato Res.* **1972,** *15*, 5.

9.   Cotter, P. A.; Stibitz, S., c-di-GMP-mediated regulation of virulence and biofilm formation. *Current opinion in microbiology* **2007,** *10* (1), 17-23.

10.   Sondermann, H.; Shikuma, N. J.; Yildiz, F. H., You've come a long way: c-di-GMP signaling. *Current opinion in microbiology* **2012,** *15* (2), 140-6.

11.   Massie, J. P.; Reynolds, E. L.; Koestler, B. J.; Cong, J. P.; Agostoni, M.; Waters, C. M., Quantification of high-specificity cyclic diguanylate signaling. *Proceedings of the National Academy of Sciences of the United States of America* **2012,** *109* (31), 12746-51.

12.   Waters, C. Cyclic di-GMP-A Newly Appreciated Bacterial Signaling Molecule.

13.   Ryjenkov, D. A.; Tarutina, M.; Moskvin, O. V.; Gomelsky, M., Cyclic diguanylate is a ubiquitous signaling molecule in bacteria: insights into biochemistry of the GGDEF protein domain. *J Bacteriol* **2005,** *187* (5), 1792-8.

14.   Chan, C.; Paul, R.; Samoray, D.; Amiot, N. C.; Giese, B.; Jenal, U.; Schirmer, T., Structural basis of activity and allosteric control of diguanylate cyclase. *Proceedings of the National Academy of Sciences of the United States of America* **2004,** *101* (49), 17084-9.

15.   Wan, X.; Tuckerman, J. R.; Saito, J. A.; Freitas, T. A.; Newhouse, J. S.; Denery, J. R.; Galperin, M. Y.; Gonzalez, G.; Gilles-Gonzalez, M. A.; Alam, M., Globins synthesize the second messenger bis-(3'-5')-cyclic diguanosine monophosphate in bacteria. *Journal of molecular biology* **2009,** *388* (2), 262-70.

16.   Gilles-Gonzalez, M. A.; Gonzalez, G., Heme-based sensors: defining characteristics, recent developments, and regulatory hypotheses. *Journal of inorganic biochemistry* **2005,** *99* (1), 1-22.

17.   Freitas, T. A.; Saito, J. A.; Hou, S.; Alam, M., Globin-coupled sensors, protoglobins, and the last universal common ancestor. *Journal of inorganic biochemistry* **2005,** *99* (1), 23-33.

18.	Aono, S., Metal-containing sensor proteins sensing diatomic gas molecules. *Dalton Trans* **2008,** (24), 3137-46.

19.	Freitas, T. A. K.; Hou, S.; Alam, M., The diversity of globin-coupled sensors. *FEBS Letters* **2003,** *552* (2–3), 99-104.

20.	Saito, J. A.; Freitas, T. A.; Alam, M., Cloning, expression, and purification of the N-terminal heme-binding domain of globin-coupled sensors. *Methods in enzymology* **2008,** *437*, 163-72.

21.	Hou, S.; Larsen, R. W.; Boudko, D.; Riley, C. W.; Karatan, E.; Zimmer, M.; Ordal, G. W.; Alam, M., Myoglobin-like aerotaxis transducers in Archaea and Bacteria. *Nature* **2000,** *403* (6769), 540-4.

22.	Tuckerman, J. R.; Gonzalez, G.; Sousa, E. H.; Wan, X.; Saito, J. A.; Alam, M.; Gilles-Gonzalez, M. A., An oxygen-sensing diguanylate cyclase and phosphodiesterase couple for c-di-GMP control. *Biochemistry* **2009,** *48* (41), 9764-74.

23.	Thijs, L.; Vinck, E.; Bolli, A.; Trandafir, F.; Wan, X.; Hoogewijs, D.; Coletta, M.; Fago, A.; Weber, R. E.; Van Doorslaer, S.; Ascenzi, P.; Alam, M.; Moens, L.; Dewilde, S., Characterization of a globin-coupled oxygen sensor with a gene-regulating function. *The Journal of biological chemistry* **2007,** *282* (52), 37325-40.

24.	Sawai, H.; Yoshioka, S.; Uchida, T.; Hyodo, M.; Hayakawa, Y.; Ishimori, K.; Aono, S., Molecular oxygen regulates the enzymatic activity of a heme-containing diguanylate cyclase (HemDGC) for the synthesis of cyclic di-GMP. *Biochimica et Biophysica Acta (BBA) - Proteins & Proteomics* **2010,** *1804* (1), 166-172.

25.	Perutz, M. F., Stereochemistry of Cooperative Effects in Haemoglobin: Haem-Haem Interaction and the Problem of Allostery. *Nature* **1970,** *228* (5273), 726-734.

26.	Zhang, W.; Phillips Jr, G. N., Structure of the Oxygen Sensor in Bacillus subtilis: Signal Transduction of Chemotaxis by Control of Symmetry. *Structure* **2003,** *11* (9), 1097-1110.

27.	Ohta, T.; Yoshimura, H.; Yoshioka, S.; Aono, S.; Kitagawa, T., Oxygen-sensing mechanism of HemAT from Bacillus subtilis: a resonance Raman spectroscopic study. *Journal of the American Chemical Society* **2004,** *126* (46), 15000-1.

28.	Paul, R.; Abel, S.; Wassmann, P.; Beck, A.; Heerklotz, H.; Jenal, U., Activation of the diguanylate cyclase PleD by phosphorylation-mediated dimerization. *The Journal of biological chemistry* **2007,** *282* (40), 29170-7.

29.	De, N.; Pirruccello, M.; Krasteva, P. V.; Bae, N.; Raghavan, R. V.; Sondermann, H., Phosphorylation-independent regulation of the diguanylate cyclase WspR. *PLoS biology* **2008,** *6* (3), e67.

30.	Wassmann, P.; Chan, C.; Paul, R.; Beck, A.; Heerklotz, H.; Jenal, U.; Schirmer, T., Structure of BeF3- -modified response regulator PleD: implications for diguanylate cyclase activation, catalysis, and feedback inhibition. *Structure* **2007,** *15* (8), 915-27.

31.	De, N.; Navarro, M. V.; Raghavan, R. V.; Sondermann, H., Determinants for the activation and autoinhibition of the diguanylate cyclase response regulator WspR. *Journal of molecular biology* **2009,** *393* (3), 619-33.

32.	Plate, L.; Marletta, M. A., Nitric oxide modulates bacterial biofilm formation through a multicomponent cyclic-di-GMP signaling network. *Molecular cell* **2012,** *46* (4), 449-60.

33.	Jenal, U.; Malone, J., Mechanisms of cyclic-di-GMP signaling in bacteria. *Annual review of genetics* **2006,** *40*, 385-407.

34.   Winter, M. B.; Herzik, M. A., Jr.; Kuriyan, J.; Marletta, M. A., Tunnels modulate ligand flux in a heme nitric oxide/oxygen binding (H-NOX) domain. *Proceedings of the National Academy of Sciences of the United States of America* **2011,** *108* (43), E881-9.

35.   Winter, M. B.; McLaurin, E. J.; Reece, S. Y.; Olea, C., Jr.; Nocera, D. G.; Marletta, M. A., Ru-porphyrin protein scaffolds for sensing O2. *Journal of the American Chemical Society* **2010,** *132* (16), 5582-3.

36.   Delgado-Nixon, V. M.; Gonzalez, G.; Gilles-Gonzalez, M. A., Dos, a heme-binding PAS protein from Escherichia coli, is a direct oxygen sensor. *Biochemistry* **2000,** *39* (10), 2685-91.

37.   Sasakura, Y.; Hirata, S.; Sugiyama, S.; Suzuki, S.; Taguchi, S.; Watanabe, M.; Matsui, T.; Sagami, I.; Shimizu, T., Characterization of a direct oxygen sensor heme protein from Escherichia coli. Effects of the heme redox states and mutations at the heme-binding site on catalysis and structure. *The Journal of biological chemistry* **2002,** *277* (26), 23821-7.

38.   Liu, N.; Xu, Y.; Hossain, S.; Huang, N.; Coursolle, D.; Gralnick, J. A.; Boon, E. M., Nitric oxide regulation of cyclic di-GMP synthesis and hydrolysis in Shewanella woodyi. *Biochemistry* **2012,** *51* (10), 2087-99.

39.   Webb, M. R., A continuous spectrophotometric assay for inorganic phosphate and for measuring phosphate release kinetics in biological systems. *Proceedings of the National Academy of Sciences of the United States of America* **1992,** *89* (11), 4884-7.

40.   Klatt, P.; Pfeiffer, S.; List, B. M.; Lehner, D.; Glatter, O.; Bachinger, H. P.; Werner, E. R.; Schmidt, K.; Mayer, B., Characterization of heme-deficient neuronal nitric-oxide synthase reveals a role for heme in subunit dimerization and binding of the amino acid substrate and tetrahydrobiopterin. *The Journal of biological chemistry* **1996,** *271* (13), 7336-42.

41.   Yoshimura, T.; Sagami, I.; Sasakura, Y.; Shimizu, T., Relationships between heme incorporation, tetramer formation, and catalysis of a heme-regulated phosphodiesterase from Escherichia coli: a study of deletion and site-directed mutants. *The Journal of biological chemistry* **2003,** *278* (52), 53105-11.

42.   Wearne, S. J., Factor Xa cleavage of fusion proteins. Elimination of non-specific cleavage by reversible acylation. *FEBS Lett* **1990,** *263* (1), 23-6.

43.   Christen, B.; Christen, M.; Paul, R.; Schmid, F.; Folcher, M.; Jenoe, P.; Meuwly, M.; Jenal, U., Allosteric control of cyclic di-GMP signaling. *The Journal of biological chemistry* **2006,** *281* (42), 32015-24.

44.   Rao, F.; Pasunooti, S.; Ng, Y.; Zhuo, W.; Lim, L.; Liu, A. W.; Liang, Z. X., Enzymatic synthesis of c-di-GMP using a thermophilic diguanylate cyclase. *Analytical biochemistry* **2009,** *389* (2), 138-42.

45.   Burns, J. L.; DiChristina, T. J., Anaerobic respiration of elemental sulfur and thiosulfate by Shewanella oneidensis MR-1 requires psrA, a homolog of the phsA gene of Salmonella enterica serovar typhimurium LT2. *Applied and environmental microbiology* **2009,** *75* (16), 5209-17.

46.   Jackson, D. W.; Suzuki, K.; Oakford, L.; Simecka, J. W.; Hart, M. E.; Romeo, T., Biofilm formation and dispersal under the influence of the global regulator CsrA of Escherichia coli. *Journal of bacteriology* **2002,** *184* (1), 290-301.

47.   Gentner, M.; Allan, M. G.; Zaehringer, F.; Schirmer, T.; Grzesiek, S., Oligomer formation of the bacterial second messenger c-di-GMP: reaction rates and equilibrium

constants indicate a monomeric state at physiological concentrations. *Journal of the American Chemical Society* **2012,** *134* (2), 1019-29.

48.	Ryan, D. E.; Wood, A. W.; Thomas, P. E.; Walz, F. G., Jr.; Yuan, P. M.; Shively, J. E.; Levin, W., Comparisons of highly purified hepatic microsomal cytochromes P-450 from Holtzman and Long-Evans rats. *Biochimica et biophysica acta* **1982,** *709* (2), 273-83.